

# Selective Voltammetric Detection of Chlorophylls Using a Semi-circular Potential Wave

Yuanzhe Wang, Lifu Chen, Richard G Compton\*

Department of Chemistry, Physical and Theoretical Chemistry Laboratory, Oxford University,  
South Parks Road, Oxford OX1 3QZ, UK

\*Corresponding author

Email: richard.compton@chem.ox.ac.uk

Phone: +44 (0) 1865 275957

Fax: +44 (0) 1865 275410

Email addresses of co-authors:

[yuanzhe.wang@wadham.ox.ac.uk](mailto:yuanzhe.wang@wadham.ox.ac.uk)

[lifu.chen@chem.ox.ac.uk](mailto:lifu.chen@chem.ox.ac.uk)

To be submitted to:

Food Chemistry

## 1 Abstract

2 A simple electrochemical method employing a novel semi-circular potential sweep voltammetry on a glassy  
3 carbon (GC) electrode was developed to distinguish and quantify two main chlorophyll components  
4 (chlorophyll a and b) present in their mixtures. The semi-circular potential sweep generates large, transient  
5 scan rates, enabling the selective detection of species with closely similar oxidative potentials. The proposed  
6 method shows good applicability in mixtures of chlorophyll a (Chl a) and chlorophyll b (Chl b) with  
7 concentrations ranging from 46.2 to 110.8  $\mu\text{M}$  and 46.2 to 92.4  $\mu\text{M}$  respectively, which were prepared to  
8 mimic varying compositions of chlorophyll a and b in nature for the application in food quality control. The  
9 method was successfully applied to real sample of spinach.

## 10 Keywords:

11 Chlorophyll

12 Semi-circular potential sweep voltammetry

13 Detection in Mixtures

## 14 1. Introduction

15 In electroanalysis, cyclic voltammetry (CV) is a widely used technique, in particular, for initial analysis of  
16 new redox systems, providing abundant information such as rate constants, formal potentials, electron  
17 transfer coefficients to study the kinetics and thermodynamics of electrochemical reactions (Bard, Faulkner,

$$E(t) = \pm vt + E(t = 0) \quad (1)$$

18 Zoski, & Leddy, 2001). It employs a linear potential waveform (Compton & Banks, 2018):

19 where the  $\pm$  sign indicates the oxidation or reduction of the studied reaction and  $v$  is the scan rate that  
20 remains constant. However, an alternative method has been proposed recently, employing a semi-circular  
21 potential wave as follows (Y. Uchida, Katelhon, & Compton, 2018a, 2018b):

$$E(t) = \pm A_0 \sqrt{\left| 1 - \left[ 2 \left( \frac{t}{t_{max}} - c \right) \right]^2 \right|} + E_{centre} \quad (2)$$

$$E_{centre} = \frac{E_f - E_i}{2} \quad (3)$$

where  $A_0$  is the amplitude of the potential wave,  $t$  is the time and  $t_{max}$  is the duration of a single scan between the two potential limits.  $c = 0$  for  $t \leq t_{max}/2$ ,  $c = 1$  for  $t_{max}/2 < t < t_{max}$  and  $E_{centre}$  is the midpoint of the applied potential window, which is experimentally defined relative to the reference electrode with the start potential  $E_i$  and the vertex potential  $E_f$ . The main features of semi-circular potential wave in contrast to conventional linear wave are that it generates an instantaneous infinite scan rate at the midpoint of the potential window and relatively slower scan rates in other regions. The current response, which is dependent on the scan rate, can thus be selectively amplified at a desired potential while compressed at others. This novel method giving significant current amplification was validated by Uchida *et al.* via simulation (Y. Uchida, Katelhon, & Compton, 2019), where its use for determining standard electrochemical rate constants,  $k_0$ , with one magnitude greater accuracy than via conventional CV was also suggested. The experimental verification of semi-circular potential sweep voltammetry was performed on the well-known redox couple  $\text{Ru}(\text{NH}_3)^{3+/2+}$ , showing good agreement with theory and a potential use in determining the formal potential (Amin, Uchida, Katelhon, & Compton, 2019).

The use of semi-circular potential sweep voltammetry for electroanalytical applications is just beginning to be investigated computationally and experimentally. The main advantage of applying a semi-circular potential wave is its ability to generate the markedly increased current response and thus improve the detection sensitivity. This was demonstrated by Uchida *et al.* in a theoretical study employing semi-circular potential sweep in stripping voltammetry designed for the adsorbed species (Y Uchida, Kätelhön, & Compton, 2019). Further, the use of semi-circular potential sweep voltammetry in experiments for a diffusion-controlled electrochemical process to obtain amplified signals facilitating simple data analysis was reported in our recent work on quantification of piperine in black pepper (Wang, Chen, Chaisiwamongkhol, & Compton, 2019).

In order to further appreciate semi-circular potential sweep voltammetry and in particular, develop it into a powerful tool for electroanalytical applications, we herein apply the semi-circular potential sweep voltammetry to the analysis of a mixture of two species. As predicted by Uchida *et al.* on the basis of computational simulation (Y. Uchida et al., 2018b), semi-circular voltammetry is advantageous over conventional CV in distinguishing two individual species from a mixture, in particular, when they have

50 closely similar peak potentials in classical CV. To demonstrate this experimentally, chlorophyll a (Chl a) and  
51 chlorophyll b (Chl b), and their closely similar redox potentials (Goedheer, Dehaas, & Schuller, 1958;  
52 Kobayashi et al., 2007; Nonomura, Igarashi, Yoshioka, & Inoue, 1997).

53 The chlorophylls are a group of tetrapyrrolic pigments involved in photosynthesis in higher plants, algae,  
54 and some species of bacteria. Chl a and Chl b are two major light-adsorbing pigments (Scheer, 1991),  
55 playing pivotal roles in the electron transfer that occurs at the reaction centres of both photosystem I and  
56 photosystem II . They are very similar in structure and found to coexist in many oxygenic photosynthetic  
57 organisms (Scheer, 1991). Both of them possess the porphyrin ring coordinating to a central magnesium ion  
58 while Chl a distinguishes from Chl b by its 7-methyl-substituent rather than 7-formyl functional group  
59 (Figure 1 (A)(B)). The chlorophylls were reported to show prooxidant activities under light, transferring the  
60 energy absorbed from light to the present triplet oxygen to form highly reactive singlet oxygen but act as  
61 antioxidants at dark conditions owing to the structure of their porphyrin rings. Chl a was found to possess a  
62 higher prooxidant activity than Chl b whereas Chl b is a stronger antioxidant (Choe & Min, 2006).

63 Due to their important roles in photosynthetic process and abundant presences in nature, determinations of  
64 chlorophylls are required for both mechanism investigations and industrial / agricultural analysis including  
65 quality control of crops (Zhang et al., 2016) and food products (Schoefs, 2003), as well as measurements of  
66 phytoplankton (Boyer, Kelble, Ortner, & Rudnick, 2009) biomasses for applications in water quality  
67 monitoring and environmental pollution assessment. In particular, for many types of edible oil products, for  
68 example and notably, extra virgin olive oil, chlorophylls and their degradation products such as pheophytins  
69 and pyropheophytins can serve as indicators of the product storage stability due to their prooxidant or  
70 antioxidant behaviours, which have clear effects on the photosensitized oxidation or autoxidation of the  
71 product (Choe & Min, 2006). Extra virgin olive oil has generally been suggested as needing to be stored in  
72 the dark to maintain its overall oxidative stability and nutritional value, preventing the degradation of some  
73 minority compounds including chlorophyll (present mainly as pheophytin a in this product) which reduces  
74 the autoxidation of the oil in the dark (Cecchi, Passamonti, & Cecchi, 2010; Silva, Anjos, Cavalcanti, &  
75 Celeghini, 2015). Light accelerates the oil oxidation by triggering the reaction of singlet oxygen via  
76 photosensitized oxidation. Packaging technologies such as applying oxygen scavengers (Cecchi, Passamonti,  
77 & Cecchi, 2010) and light filtering packaging materials (Trypidis et al., 2019) can help better maintain the  
78 quality of oil under light, although they may become less effective when high concentrations of chlorophyll

79 as prooxidant are present (Trypidis et al., 2019). Moreover, pyropheophytins have been reported to be very  
80 sensitive to temperature, another factor affecting the shelf-life of extra virgin olive oil, therefore these  
81 molecules can be used as a freshness parameter indicating exposure to temperature changes over 25°C  
82 (Conte et al., 2020).

83 Among a variety of techniques for chlorophyll identification and quantification, spectrophotometry (Ergun,  
84 Demirata, Gumus, & Apak, 2004), UV-vis (Vernon & Seely, 1966) and fluorescence (Maxwell & Johnson,  
85 2000) spectroscopy are most commonly used for routine detections, offering good specificity and sensitivity  
86 based on their characteristic light-absorbing/emitting properties. Nonetheless, electrochemical methods are  
87 potentially a facile and accurate replacement of the spectroscopic methods and have also been studied  
88 extensively on gold (Khanova & Tarasevich, 1987), mercury (Agostiano, Cosma, & Dellamonica, 1990),  
89 platinum (Suponeva, Kazakova, & Kisselev, 1989), SnO<sub>2</sub> (Yang, Zhou, Han, & Jiang, 1994) electrodes as  
90 well as carbon electrodes (Nonomura et al., 1997; cPemberton, Amine, & Hart, 2004; Suponeva,  
91 Hotchandani, Arbour, & Kisselev, 1996) using cyclic voltammetry and more sensitive electroanalytical  
92 techniques including adsorptive stripping voltammetry (AdSV), differential pulse voltammetry (DPV) and  
93 square wave voltammetry (SWV). For the structurally similar Chl a and Chl b, the similar square wave  
94 voltammograms were found (Kobayashi et al., 2007) and close redox potential values of them were reported  
95 (Goedheer et al., 1958; Kobayashi et al., 2007) at platinum electrode in non-aqueous media. While most of  
96 the studies focus on merely the mechanistic interpretations of chlorophylls, Pemberton *et al.* reported the  
97 electro-oxidation behaviours of Chl a using screen-printed carbon electrode and developed an approach for  
98 its detection in cow faeces (Pemberton et al., 2004). However, the aforementioned electrochemical studies all  
99 focus on either the singular chlorophyll determination or simply the total chlorophyll (a+b) mixture, Chl a  
100 and Chl b have not been distinguished electrochemically in the mixture resulting from direct extraction from  
101 common green vegetables. Developing a simple, rapid and sensitive method to detect and distinguish the  
102 structurally similar Chl a and Chl b that possess different properties, like prooxidant/antioxidant capabilities,  
103 is crucial for performing quantitative analysis of each substance and accurately evaluating the qualities of  
104 mixtures in industry, which may also be meaningful when consider the detections of other similar  
105 compounds such as pheophytins and pyropheophytins.

106 In this work, we present an electroanalytical method employing semi-circular potential sweep voltammetry  
107 to distinguish and quantify two structurally similar compounds in a mixture. First, the electrochemical  
108 behaviour of Chl a and Chl b are investigated using cyclic voltammetry on a GC electrode. The applicability  
109 of the developed method using semi-circular potential sweep voltammetry in detecting Chl a and Chl b  
110 individually in a 1:1 mixture is next demonstrated. Finally, its potential application in determining the  
111 chlorophyll content of a spinach sample is suggested.

## 112 **2. Experimental**

### 113 **2.1 Chemicals and Reagents**

114 Chlorophyll a and b were extracted and partially purified from fresh spinach leaves based on a previously  
115 published method (Iriyama & Shiraki, 1979), followed by subsequent purification performed on a silica gel  
116 column chromatography using 60 Å silica gel 40-63 µm purchased from VWR. A detailed procedure of  
117 extraction and column chromatography purification is fully described in Section 1 of the Supporting  
118 Information. The spinach was purchased fresh from a local supermarket (Tesco, Oxford, UK). The products  
119 of Chl a and Chl b obtained from 100 g spinach were weighed as 22.3 mg and 6.2 mg and dissolved in  
120 acetone or diethyl ether for further measurements. Stock solutions in acetone were stored in the dark at -  
121 19 °C. The purity and concentration of samples were routinely checked by UV-vis spectroscopy in ether  
122 solutions. All other chemicals were of analytical grade and were used received without any further  
123 purification. The chlorophyll solutions were prepared with acetone (≥99.8%) and diethyl ether (≥99.8%)  
124 purchased from Sigma-Aldrich. All solutions for electrochemical measurements were prepared with  
125 deionised water at a resistivity of 18.2 MΩ cm at 298K (Millipore, MA, USA). The phosphate-buffered  
126 saline (PBS, 1×, pH=7.4) was prepared using sodium chloride (137 mM, ≥99.5%), potassium chloride (2.7  
127 mM, ≥99.0%), sodium phosphate dibasic (10 mM, ≥99.0%), and potassium phosphate monobasic (1.8 mM,  
128 ≥99.0%), purchased from Sigma-Aldrich.

### 129 **2.2 Apparatus**

130 UV-vis spectroscopy was conducted using a Shimadzu spectrometer UV-1800 and quartz cells with a 10  
131 mm optical path. The absorbance was recorded from 800– 300 nm and a baseline correction was conducted  
132 prior to all measurements.

133 All electrochemical experiments were conducted with a standard three-electrode system in a Faraday cage  
134 at 298K. The cyclic voltammetric measurements were performed using a  $\mu$ Autolab II potentiostat (Metrohm-  
135 Autolab BV, Netherlands). Semi-circular potential wave sweep voltammetry was carried out with a  
136 computer-controlled in-lab built potentiostat ensuring the low-noise measurements with signal sampled at a  
137 stream rate of 100 kHz (Amin et al., 2019). The potentiostat was controlled by script written in Python 3.5 to  
138 generate required potential waveform. For the voltammetric measurements, a glassy carbon (GC)  
139 macroelectrode (diameter calibrated as 2.99 mm) was used as the working electrode, a saturated calomel  
140 electrode (SCE, ALS distributed by BASi Inc., Japan.) as the reference electrode and a graphite rod as the  
141 counter electrode. The GC electrode was polished onto the soft lapping pads (Buehler, UK) with alumina  
142 (particles size of 1.0 and 0.3  $\mu$ m, Buehler, IL, UK) before each voltammetric experiment, followed by  
143 sonication in water and drying with nitrogen.

## 144 2.3 Analytical Procedure

145 The purities of Chl a and Chl b fractions obtained from column chromatography were first examined in  
146 ether solutions using UV-vis spectroscopy. The spectral absorption properties (adsorption peak shapes,  
147 adsorption maxima and band ratios) shown on the UV-vis spectras (Figure S1) of Chl a and Chl b were  
148 compared with the values reported in literature (Section 2 in Supporting Information). Chl a and Chl b were  
149 next resolubilised in acetone and prepared as stocking solutions (370  $\mu$ M). The concentrations of Chl a and  
150 Chl b solutions in acetone were determined using UV-vis spectroscopy. The stock solutions were then  
151 diluted to the concentrations of 1.45–111  $\mu$ M as standard working solutions.

152 All experiments were conducted under dim light and solution was bubbled with N<sub>2</sub> for 10 minutes to  
153 remove dissolved oxygen before each measurement. The chlorophyll standard mixture solutions are prepared  
154 by adding increasing concentrations of Chl a or Chl b from 9.24–64.6  $\mu$ M to a 1:1 mixture containing 46.2  
155  $\mu$ M Chl a and Chl b. For cyclic voltammetric and semi-circular potential sweep voltammetric experiments  
156 using the standard solutions, the GC electrode was immersed in the Chl a and / or Chl b acetone solutions for

one minute to allow the adsorption of chlorophyll onto the electrode surface. The electrode was then gently rinsed with deionised water and transferred to the blank degassed PBS solution at pH 7.4 for voltammetric measurements.

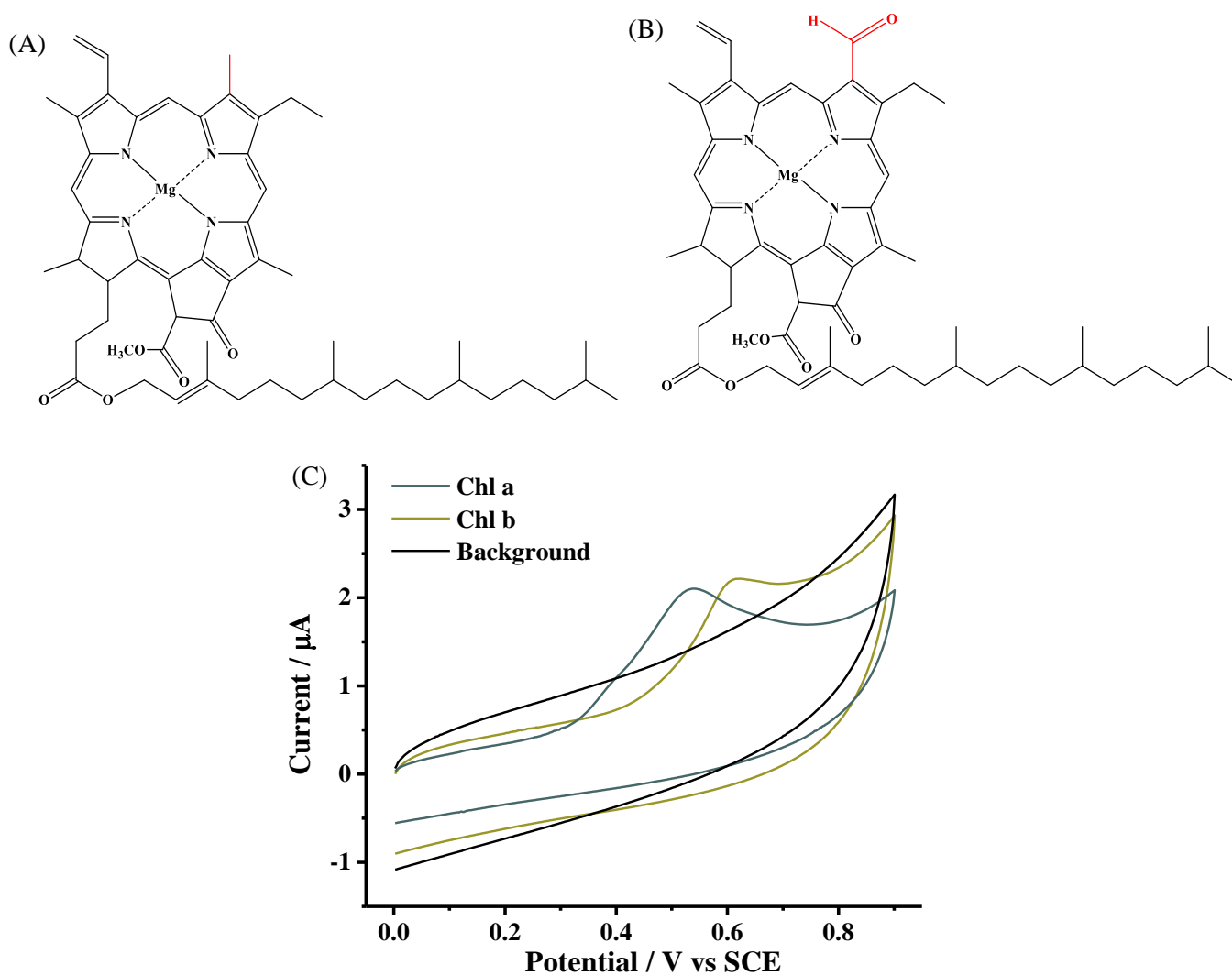
For real sample analysis, the yielded crude product from the extraction of spinach without column chromatographic purification was diluted with acetone until the voltammetric responses fell within the linear detection range (dilution factor =50) and used for the initial cyclic voltammetric and semi-circular voltammetric tests. The same electrode preparation procedure was used as above. The Chl a standard solutions in the concentration range of 23.1–80.9  $\mu\text{M}$  were then added to the crude for quantification in real samples using semi-circular potential sweep voltammetry.

### 3. Results and Discussion

In the following sections, first, the electrochemical behaviour of Chl a and Chl b separately adsorbed on a GC electrode are studied and compared using CV. Next, semi-circular potential sweep voltammetry is employed for selective detection of Chl a and Chl b in a 1:1 mixture of them, as well as compared to the conventional CV method. The potential window is optimised to give the best resolution of chlorophyll peaks in mixture detection and used for the standard additions analysis of Chl a and Chl b. Finally, standard additions of Chl a to a real sample of spinach is conducted for application in food quality control.

173 3.1 Electrochemical behaviours of chlorophylls

174 3.1.1 Effect of Scan rates



175 Figure 1. Chemical structures and electrochemical signals: Chemical structures of (A) chlorophyll a and (B) chlorophyll b. (C) Cyclic  
 176 voltammetric responses of background, 23.1  $\mu\text{M}$  Chl a and Chl b at GC electrode measured in PBS under degassed condition. Scan  
 177 rate= 100  $\text{mV s}^{-1}$

178 The voltammetric behaviour of Chl a and Chl b separately on a GC electrode were first investigated using  
 179 conventional cyclic voltammetry. The GC electrode was immersed in 23.1  $\mu\text{M}$  of Chl a or 11.6  $\mu\text{M}$  of Chl b  
 180 solutions for one minute before being transferred to a degassed PBS solution. Cyclic voltammetric responses  
 181 of Chl a and Chl b were recorded at a scan rate of 100  $\text{mV s}^{-1}$ , showing an irreversible oxidation peak at  
 182 +0.54V vs. SCE for Chl a and another irreversible oxidation peak at +0.62 V vs. SCE for Chl b in the chosen  
 183 potential window (Figure 1(C)). As can be seen, the voltammograms of the two chlorophylls appeared to be  
 184 closely similar at GC electrode, except that the oxidation of Chl b is shifted to a slightly more positive  
 185 potential, which reflects the change of a  $-\text{CH}_3$  substituent group (Chl a) to an electron withdrawing group –

186 CHO (Chl b) reducing the electron density of chlorophyll  $\pi$ -conjugated system (Falk & Smith, 1975; Scheer,  
187 1991).

188 To confirm the adsorption of Chl a and Chl b onto GC electrode surface, the effects of scan rate on the  
189 oxidation peak currents were studied. Figure 2(A) and (B) depicts the cyclic voltammograms of Chl a and  
190 Chl b recorded at the scan rates in the range of 25 to 400 mVs<sup>-1</sup>. Linear relationships between peak currents  
191 and scan rates were found for both compounds from 25 to 400 mVs<sup>-1</sup> (Insets of Figure 2(A) and 2(B)),  
192 suggesting the observed oxidations of Chl a and Chl b are both surface bound processes.

### 193 3.1.2 Adsorption on GC electrode

194 Having identified the chlorophyll electrochemistry as from surface-confined species, the adsorption of the  
195 chlorophylls on GC electrode surface was next investigated. Cyclic voltammetry of Chl a at varying  
196 concentrations was performed with an immersion time of one minute, which was experimentally determined  
197 to be the minimum time required for the voltammetric peak areas to reach a plateau and so leading to a  
198 sensitive and reproducible detection of the chlorophylls (Section 3 in Supporting Information). The cyclic  
199 voltammetric responses of Chl a in the concentration range of 1.45–370  $\mu$ M, at a scan rate of 100 mVs<sup>-1</sup> were

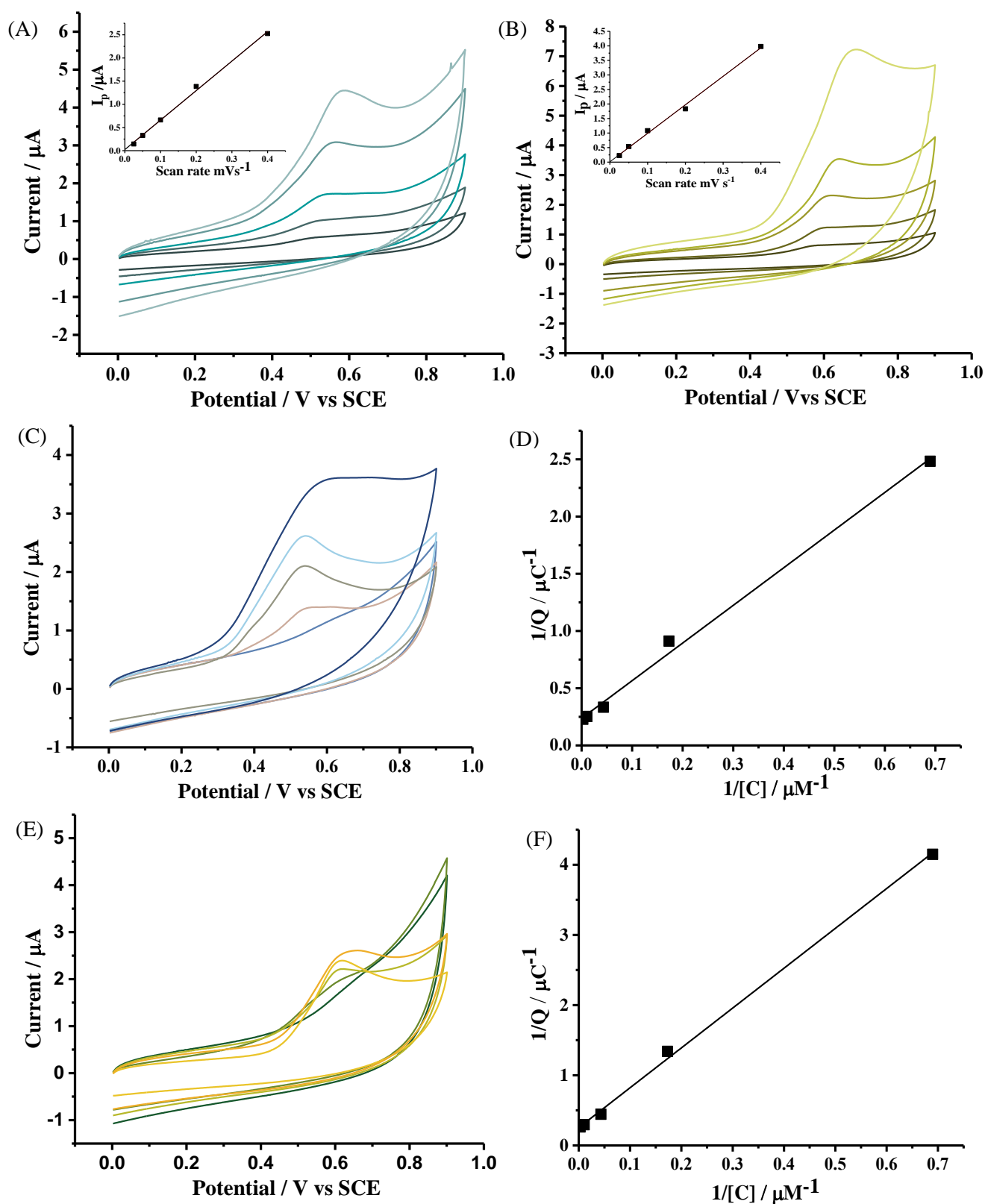
$$\theta = \frac{K[C]}{1 + K[C]} \quad (4)$$

200 recorded in Figure 2(C), which was analysed with Langmuir isotherm according to the following equation:

201 where  $\theta$  is the fractional occupancy of the adsorption sites,  $K$  is the equilibrium constant for adsorption and  
202  $[C]$  is the concentration of Chl a. Eq. (4) can be rewritten as:

$$\frac{1}{Q} = \left( \frac{1}{KQ_{max}} \right) \left( \frac{1}{[C]} \right) + \frac{1}{Q_{max}} \quad (5)$$

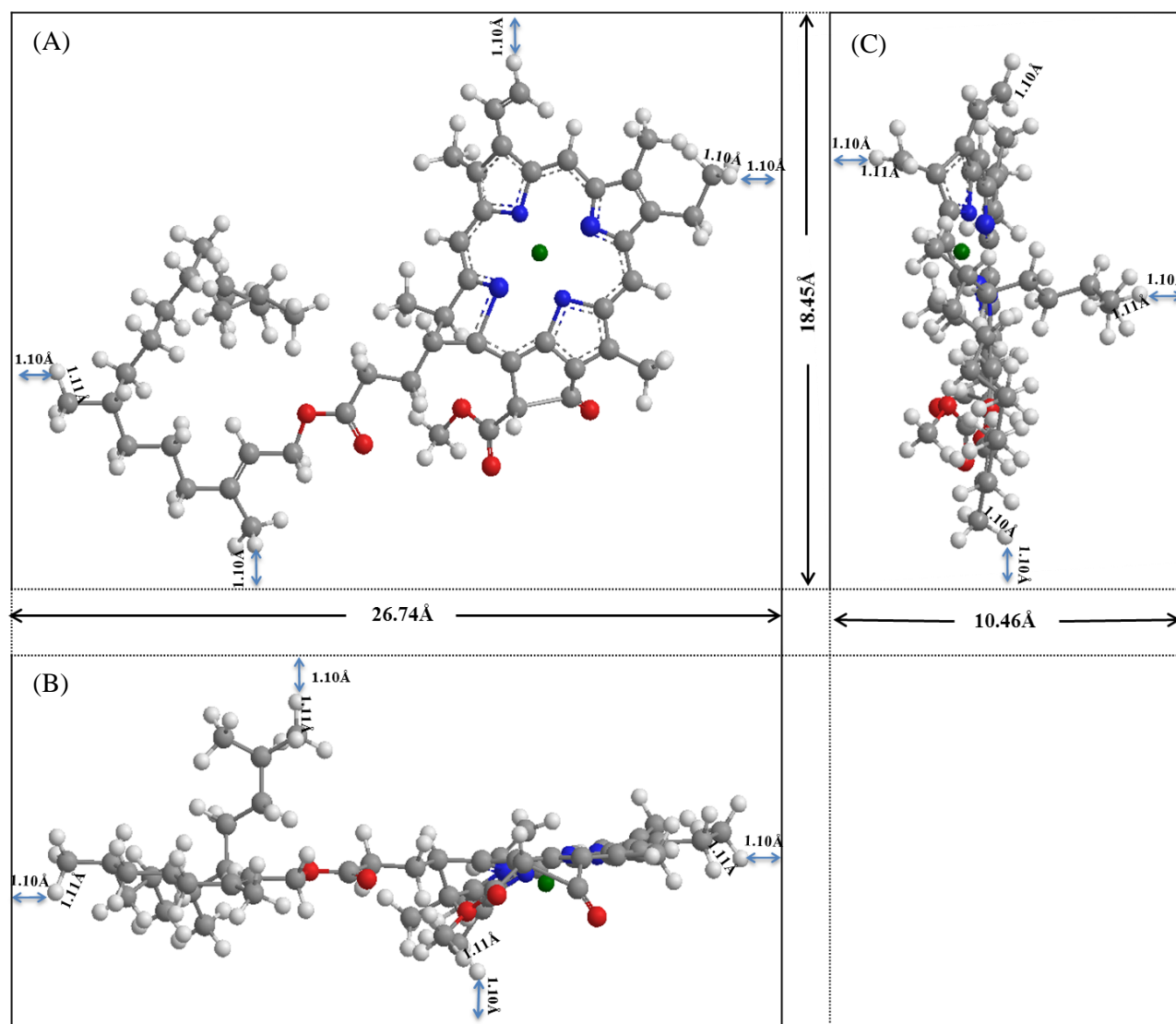
203 where  $Q$  is the voltammetrically measured charge transferred during oxidation of the species at the studied  
204 concentrations and  $Q_{max}$  is maximum charge transfer at saturation of the surface with Chl a. The Langmuir  
205 plot shown in Figure 2(D) exhibits a linearity ( $1/Q$  ( $\mu$ C<sup>-1</sup>) = (3.290 $\pm$ 0.119)  $1/C$  ( $\mu$ M<sup>-1</sup>) + (0.237  $\pm$  0.0378),  
206  $R^2=0.996$ ), suggesting the Chl a adsorption is well-described by the Langmuir isotherm. The equilibrium  
207 constant  $K$  and maximum charge transfer  $Q_{max}$  were calculated to be 0.072  $\mu$ M<sup>-1</sup> and 4.2  $\mu$ C, respectively.



208 Figure 2. Electrochemical behaviours of chlorophylls: Cyclic voltammetric responses of (A) 11.6  $\mu M$  Chl a oxidation and (B) 23.1  
 209  $\mu M$  Chl b at GC electrode in PBS at varying scan rates of 25  $mV s^{-1}$ , 50  $mV s^{-1}$ , 100  $mV s^{-1}$ , 150  $mV s^{-1}$ , 200  $mV s^{-1}$ , 400  $mV s^{-1}$ , under  
 210 degassed condition. Inset: plot of peak current versus scan rate; increasing concentrations from 1.45-370  $\mu M$  of (C) Chl a and (E) Chl  
 211 b at GC electrode in PBS. Langmuir plot of (D) 1.45-370  $\mu M$  Chl a using peak area obtained from (C) and (F) 1.45-370  $\mu M$  Chl b  
 212 using peak area obtained from (D).

213 In order to estimate the approximate area of a Chl a molecule adsorbed on GC, the theoretical areas of the  
 214 molecule in all three possible flat molecular orientations were calculated using the rectangular box model  
 215 presented in Scheme 1. All side lengths were estimated by trigonometry for bond lengths, bond angles and

216 van der Waals radii of the terminating atoms. The bond length, bond angles data were obtained from  
 217 ChemDraw 16.0 software and the van der Waals radii of the terminating atoms values are those tabulated by  
 218 Rowland (Batsanov, 2001). This method has been reported in several previous studies for other organic  
 219 molecules (Chen, Tanner, Lin, & Compton, 2018; Chen, Li, Tanner, & Compton, 2017). Scheme 1 shows the  
 220 flat view (A), edgewise view (B) and endwise view (C) of Chl a adsorption on GC electrode and the  
 221 corresponding areas  $A_{fl}$ ,  $A_{ed}$ ,  $A_{en}$  can be estimated as  $4.93$ ,  $2.80$ ,  $1.93 \times 10^{-14} \text{ cm}^2$ . The number of molecules  
 222 adsorbed on electrode surface ( $N_{ads}$ ) can be calculated using  $N_{ads} = A_{electrode} / A_{chl-a}$ , where  $A_{electrode}$  is the  
 223 electroactive surface area and  $A_{chl-a}$  corresponds to  $A_{fl}$ ,  $A_{ed}$  or  $A_{en}$ . However, the electroactive surface area can  
 224 deviate substantially from the geometric area of electrode and greatly depends on the surface roughness  
 225 factor, which is reported as ranging from 1.7 to 4.1 for the GC electrode (Murray, 1992). Thus  $A_{electrode}$  can be



226 Scheme 1. Rectangular box model of Chl a molecule for (A) flat view, (B) edgewise view and (C) endwise view

227 estimated as 0.12–0.29 cm<sup>2</sup> and the maximum charge transfer  $Q_{max}$  for three possible molecular orientations  
 228 can be calculated using  $N_{ads}$  and electron fundamental charge  $e$  ( $1.602 \times 10^{-19}$  C) by  $Q_{max} = N_{ads} \times e$ .  
 229 Assuming close-packed, monolayer adsorption and a two electron transfer process, the maximum charge  
 230 transfer for three molecular orientations  $Q_{fl}$ ,  $Q_{ed}$  and  $Q_{en}$  were calculated to lay in the ranges of 0.78–1.9  $\mu$ C,  
 231 1.4–3.3  $\mu$ C, 2.0–4.8  $\mu$ C, respectively. Since the experimental  $Q_{max}$  values obtained from Figure 2(D) falls  
 232 into the range of  $Q_{en}$ , it can be inferred that the Chl a adsorption follows the orientation of the endwise views  
 233 (Scheme 1(C)).

234 Following the same procedure, voltammetric responses of Chl b at the same concentration range of 1.45–  
 235 370  $\mu$ M were shown in Figure 2(E). The double reciprocal plot in Figure 2(F) again shows linearity ( $1/Q$   
 236 ( $\mu$ C<sup>-1</sup>) = (5.679 $\pm$ 0.120)  $1/C$  ( $\mu$ M<sup>-1</sup>) + (0.254  $\pm$  0.0383),  $R^2=0.998$ ), as predicted by Langmuir isotherm,  
 237 giving an equilibrium constant as 0.045  $\mu$ M<sup>-1</sup> and the maximum charge transfer as 3.9  $\mu$ C. The maximum  
 238 charge transfers of Chl b and Chl a were found to be very close in values. Since they possess closely similar  
 239 molecular structures and thus similar surface areas, it can be inferred that the adsorption of Chl b on a GC  
 240 electrode is similar to that suggested above for Chl a.

## 241 3.2 Detection of Chlorophyll a and b in Mixtures

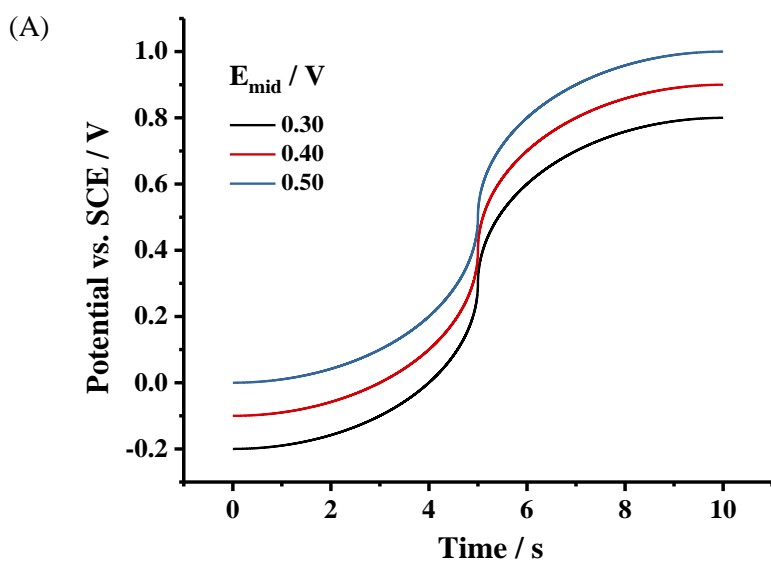
### 242 3.2.1 Selective Detection in Standard Mixture Solutions

243 Semi-circular potential wave with an average scan rate of 100 mVs<sup>-1</sup> (Figure 3(A)) was employed for the  
 244 electrochemical identification and quantification of Chl a and Chl b in the two component mixture owing to  
 245 its capacity for distinguishing two species with similar redox potentials (Y. Uchida et al., 2018b). The GC  
 246 electrode was prepared with the same procedure as above for CV and measured in PBS solution (pH =7.4).  
 247 The semi-circular potential sweep voltammograms of backgrounds and a 1:1 mixture solution containing  
 248 46.2  $\mu$ M Chl a and Chl b at varying potential windows are shown in Figure 3(B). The influence of the  
 249 adjustment of potential windows by moving the centre of the sweep relative to the potential of maximum  
 250 current was discussed in previous work (Amin et al., 2019; Wang et al., 2019). By approximating the  
 251 midpoint of potential window  $E_{centre}$  ( $E_{mid}$ ) to the oxidative potential of the studied compounds, maximum  
 252 peak currents can be obtained. As depicted in Figure 5, a set of broad peaks can be observed in the presence  
 253 of a Chl (a + b) mixture, as well as an additional very sharp peak near  $E_{centre}$ , where the infinite temporary

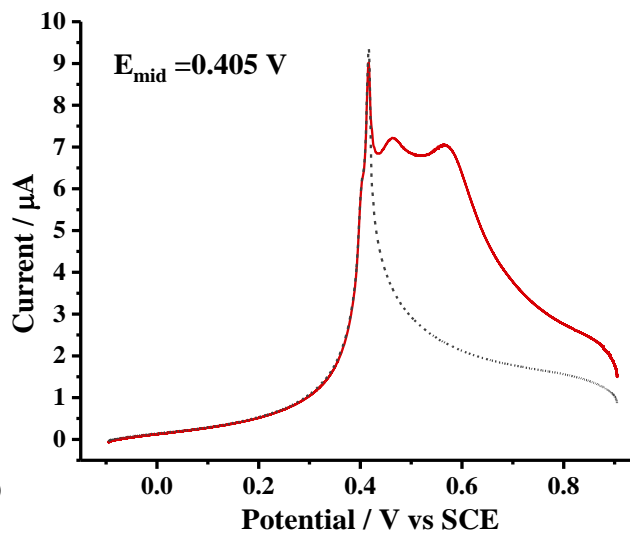
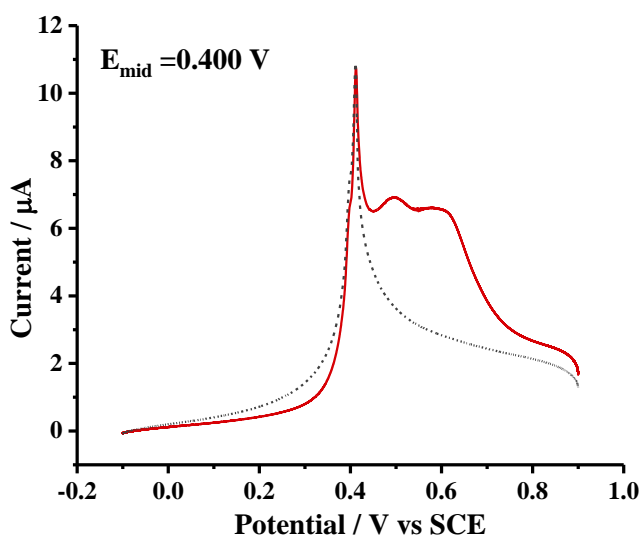
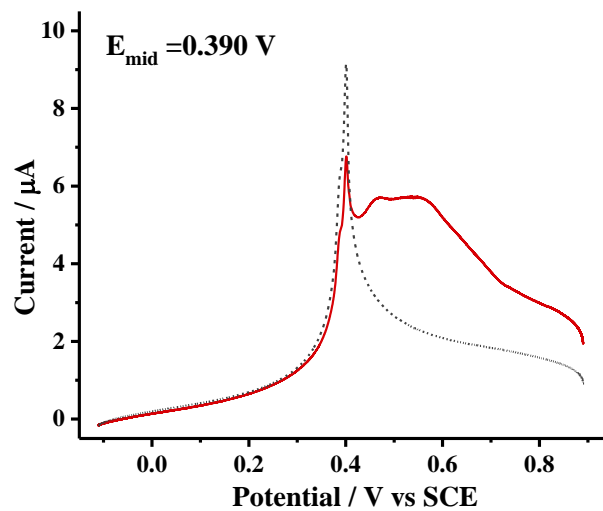
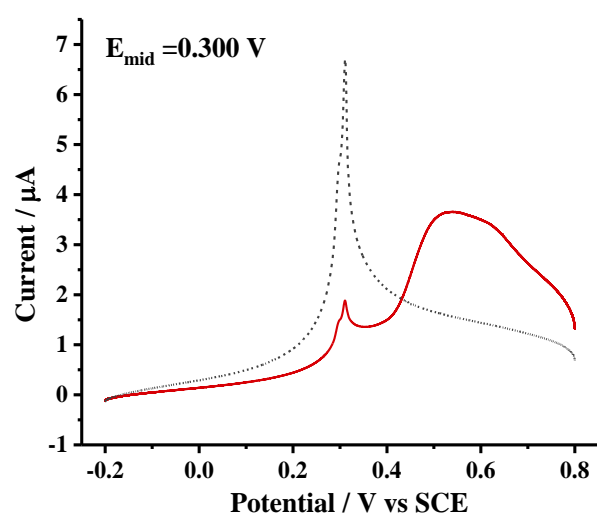
scan rate is generated. With the shift of potential windows towards the more positive  $E_{centre}$ , both of the broad peaks increase in amplitude, while the second peak grows more rapidly and the resolution of two broad peak in voltammograms improves with increasing peak separations until  $E_{centre}$  reached +0.405 V, two distinct peaks can be seen at +0.46 V and +0.57 V. From  $E_{centre} = 0.410$  V, two peaks began to decrease in resolution and finally merged with the sharp peak at  $E_{centre} = +0.500$  V. As for the sharp peak, it continually grew with the increase of positive potentials, suggesting the possible contributions from the capacitive current.

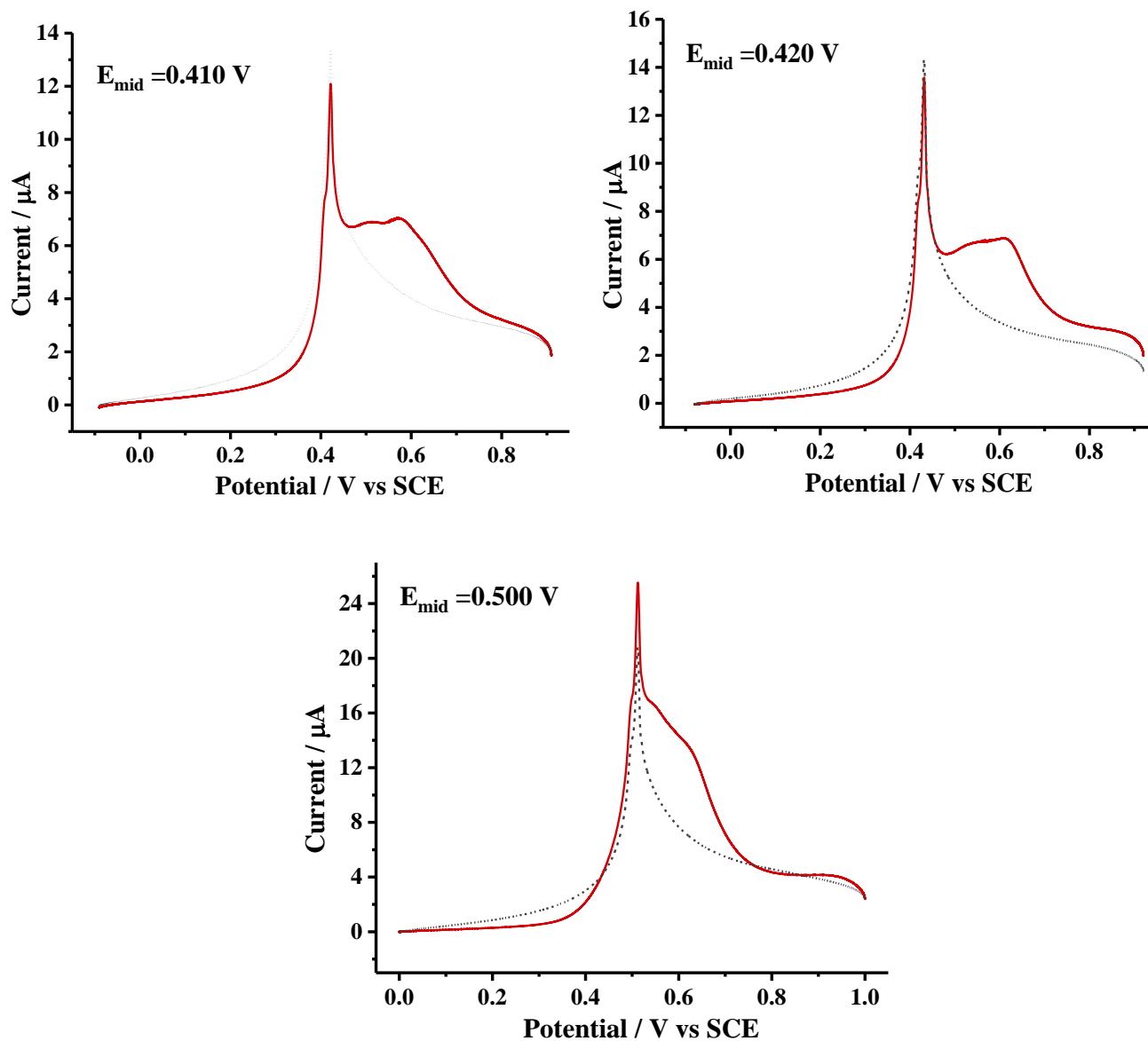
The semi-circular potential sweep voltammetric responses of both Chl a and Chl b were recorded separately in the potential window of  $E_{centre} = +0.405$  V and compared with the mixture voltammogram (Figure 4(A)). The two peaks present in the mixture voltammogram were found at the similar peak positions in the case of the isolate components, thus they can be identified as successfully recorded Chl a and Chl b peaks. The recorded semi-circular voltammograms with a potential window applied at  $E_{centre} = +0.405$  V showed excellent repeatability in the detection of mixtures, giving stable oxidation signals of Chl a and Chl b that can be measured for both singular components and mixtures with peak potential within a few millivolts.

Figure 4(B) compares the conventional cyclic voltammetric responses with the semi-circular voltammetric responses at the same average scan rate ( $100 \text{ mVs}^{-1}$ ) under the optimised potential window. It can be seen that using the semi-circular potential wave, the peak currents gained significant amplifications in the region near  $E_{centre}$  with the large, transient scan rates changing within the sweep, making the Chl a and Chl b peaks clearly distinguishable within the 1:1 mixture, in stark contrast the cyclic voltammogram shows no clear separation of the peaks due to the closeness of the oxidation potentials of two species. Thus the semi-circular voltammetry was seen to be more advantageous for the selective detection in mixtures. It was used for further quantifications of chlorophyll mixtures at the optimised potential window with  $E_{centre} = +0.405$  V, as next discussed.

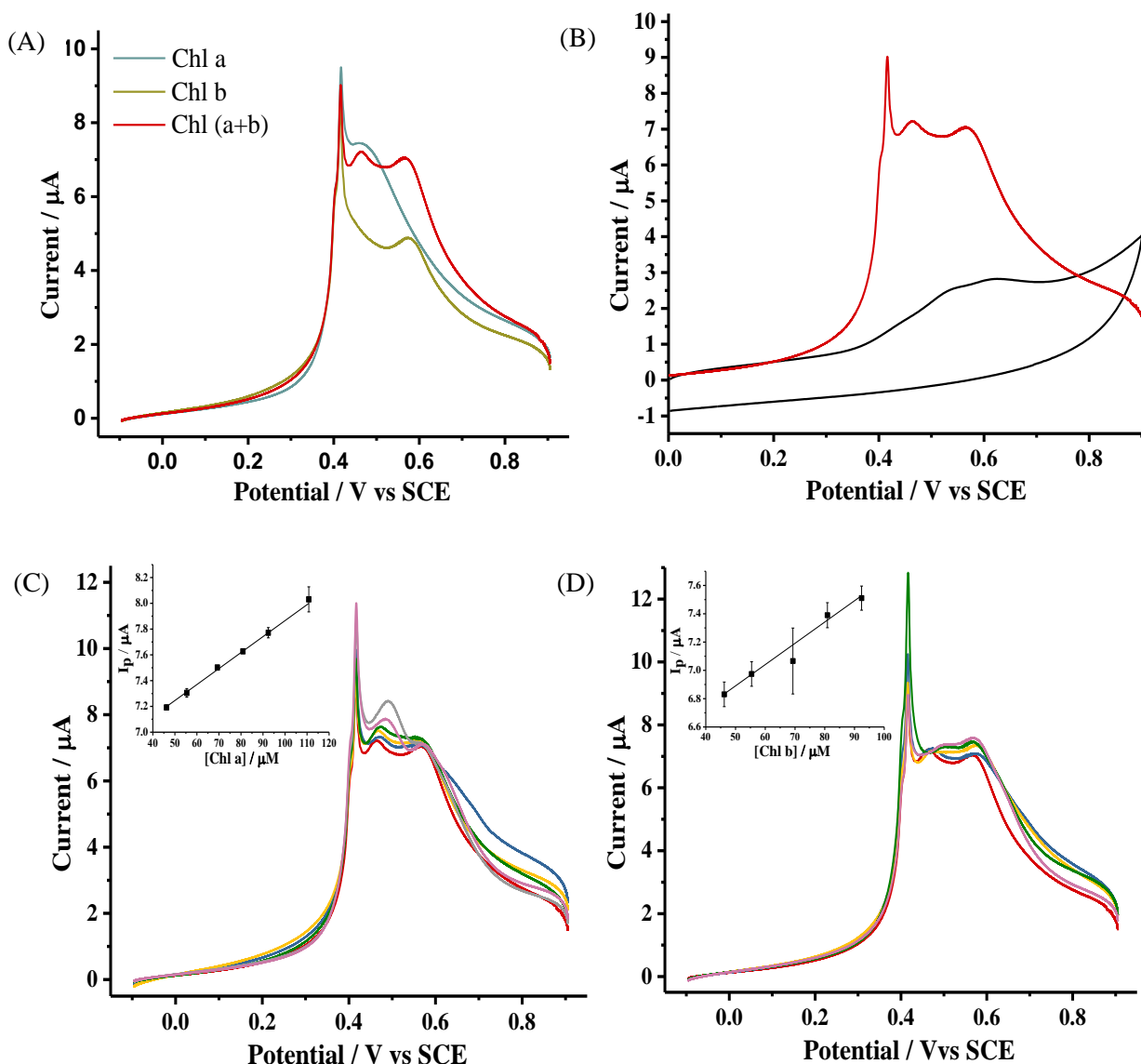


(B)





277 Figure 3. Semi-circular potential sweep voltammetry settings: Semi-circular potential (A) waveforms applied for varying  $E_{\text{centre}}$ . (B)  
 278 voltammetric responses of 0  $\mu\text{M}$  and 46.2  $\mu\text{M}$  of 1:1 Chl a: Chl b mixture solution at varying potential windows. The average of scan  
 279 rate was  $100 \text{ mVs}^{-1}$ . The scan amplitude was 0.5 V.



280 Figure 4. Semi-circular potential sweep voltammetry for the chlorophyll system: Semi-circular potential sweep voltammetric  
 281 responses at the potential window with  $E_{centre} = +0.405$  V of (A) 46.2  $\mu\text{M}$  of Chl a, Chl b and 1 standard additions of (B) 46.2  $\mu\text{M}$   
 282 1:1 Chl a: Chl b mixture in comparison to cyclic voltammogram (black line) of 46.2  $\mu\text{M}$  1:1 Chl a: Chl b mixture; standard additions  
 283 of (C) 0-64.6  $\mu\text{M}$  of Chl a and (D) 0-46.2  $\mu\text{M}$  of Chl b to a 46.2  $\mu\text{M}$  1:1 Chl a: Chl b mixture solution. The insets of (C): Plot of  
 284 currents read at +0.47 V increase with Chl a concentration in the range of 46.2-110.8  $\mu\text{M}$ ; (D): Plot of currents read at +0.57 V  
 285 increase with Chl b concentration in the range of 46.2-92.4  $\mu\text{M}$ . The average scan rate was 100  $\text{mVs}^{-1}$ .

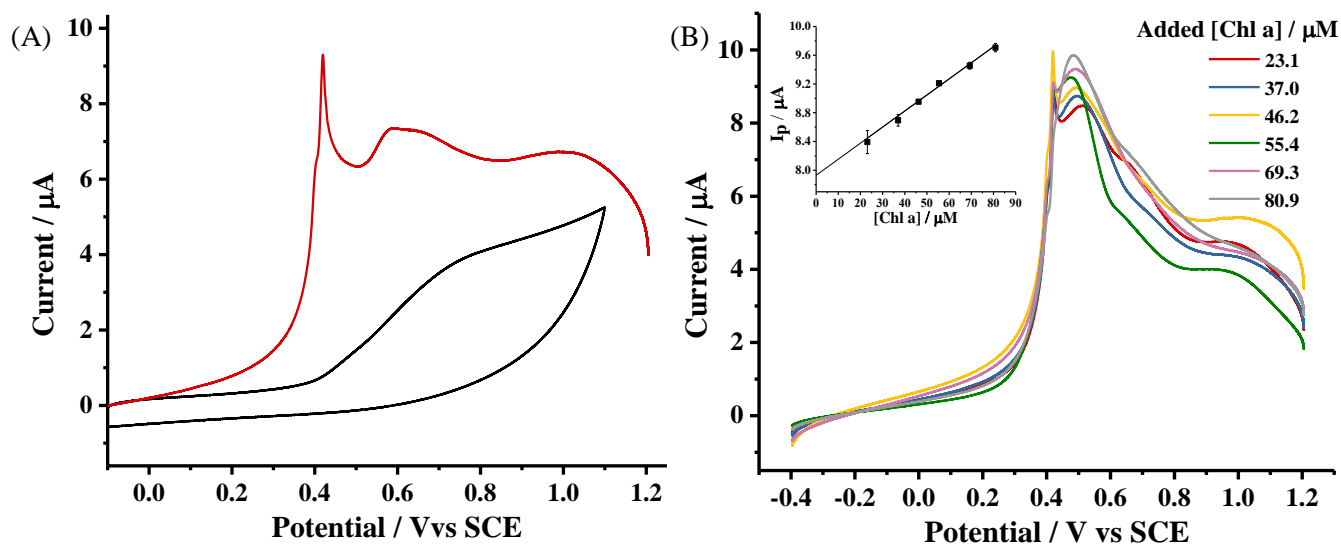
286 The validated method was applied first for the detection of standard mixture solutions containing varying  
 287 concentrations of Chl a and Chl b. The solutions were prepared by standard addition of Chl a or Chl b  
 288 solutions to an initial 1:1 mixture containing a total 46.2  $\mu\text{M}$  Chl (a + b) and adsorbed on the GC electrode  
 289 using the procedure reported above, the voltammetry was then measured in PBS solution ( $\text{pH} = 7.4$ ). Three  
 290 scans were conducted for each Chl a or Chl b concentration and the electrode was polished prior to each scan.

291 The semi-circular potential sweep voltammetric responses were recorded as a function of the concentrations  
 292 of Chl a (Figure 4 (C)) and Chl b (Figure 4 (D)). The currents resulting from Chl a standard addition were  
 293 measured at a fixed potential of +0.47 V and found to exhibit a linear relationship in the concentration range  
 294 of 46.2–111 μM (Figure 4 (C) inset,  $I_p/\mu A = (1.24 \times 10^{-2} \pm 3.12 \times 10^{-4}) [\text{Chl a}] (\mu M) + (6.63 \pm 2.43 \times 10^{-2})$   
 295  $(\mu A)$ ,  $N=6$ ,  $R^2=0.997$ ). Linear behaviour was also obtained for currents recorded at the fixed potential of  
 296 +0.57 V for the analysis of Chl b standard addition. In the range of 46.2–92.4 μM,  $I_p/\mu A = (1.50 \times 10^{-2} \pm 8.88$   
 297  $\times 10^{-4}) [\text{Chl b}] (\mu M) + (6.14 \pm 6.33 \times 10^{-2}) (\mu A)$ ,  $N=5$ ,  $R^2=0.990$  (Figure 4 (D) inset). It can be seen that the  
 298 currents read at the chosen potentials near Chl a and Chl b peaks increase linearly with the standard additions  
 299 of each component. Good reproducibility was obtained between separate experiments and sequential  
 300 voltammetric measurements (see error bars in Figures 4 and 5), allowing analysis of the mixture and  
 301 suggesting semi-circular potential sweep voltammetry is a useful analytical technique in selective detection  
 302 and quantification of individual species within a mixture of them.

### 303 3.2.2 Detection in Real Samples

304 In order to access the full applicability of developed method for mixture detection, chlorophyll  
 305 determination in a real sample was next investigated. As is general for common green plants, the spinach  
 306 crude product obtained from the mentioned extraction procedure (Section 1 in Supporting Information)  
 307 without purifying by column chromatography contains several pigment components including carotenoids  
 308 (carotenes and xanthophylls), chlorophylls (Chl a and Chl b) and pheophytins (pheophytin a and b).  
 309 Nonetheless, Chl a is the most abundant pigment consisting of ca. 58%–75% of the total pigments in spinach  
 310 (Khachik, Beecher, & Whittaker, 1986; Kidmose, Edelenbos, Christensen, & Hegelund, 2005). Therefore,  
 311 we sought to detect Chl a content selectively in the mixture of crude extract as a measure for spinach quality  
 312 control. Cyclic voltammetry and semi-circular voltammetry were first performed for the diluted spinach  
 313 extract at the average scan rate of 100 mVs<sup>-1</sup> using the potential window with the optimised  $E_{\text{centre}}$  value of  
 314 +0.405 V. From Figure 5 (A), two main peaks arising from analyte can be observed in semi-circular  
 315 voltammogram, which merged as one broad peak in cyclic voltammogram, again suggesting that the semi-  
 316 circular voltammetry can provide improved resolution and accuracy in mixture detection.

317 To identify the Chl a peak in extract voltammogram and quantify the Chl a contents in spinach, the extract  
 318 sample was next 'spiked' with Chl a standard solutions. The semi-circular potential sweep voltammetric  
 319 responses of the spiked solutions with addition of Chl a in the concentration range of 23.1–80.9  $\mu\text{M}$  was  
 320 depicted in Figure 5 (B). A linear relationship was established between currents read at +0.49 V and the  
 321 concentration of Chl a:  $I_p/\mu\text{A} = (2.24 \times 10^{-2} \pm 1.30 \times 10^{-3}) [\text{Chl a}] (\mu\text{M}) + (7.93 \pm 7.12 \times 10^{-2}) (\mu\text{A})$ ,  $N=6$ ,  
 322  $R^2=0.987$ ) (Figure 5 (B) Inset). The Chl a concentration in the spinach extract can be determined as ca. 105  
 323  $\mu\text{M}$  from the intercept of Figure 5 (B) inset combined with the linear expression in Inset of Figure 4 (C).  
 324 This can be converted into the Chl a content in fresh, raw spinach as ca. 235 mg / kg and can be estimated as  
 325 ca. 188–259 mg / kg dry matter using the spinach moisture content of 89%-92% (EngineeringToolBox, 2003;  
 326 Isleroglu, Sakin-Yilmazer, Kemerli-Kalbaran, Uren, & Kaymak-Ertekin, 2017), consistent with the Chl a  
 327 fraction weighed after column chromatography and the Chl a contents reported in the literature using HPLC  
 328 method (Lopez-Ayerra, Murcia, & Garcia-Carmona, 1998).



329 Figure 5. Semi-circular potential sweep voltammetry for the real sample: Semi-circular potential sweep voltammetric responses at the  
 330 potential window with  $E_{\text{centre}} = +0.405$  V of (A) the real sample extracted from spinach in comparison to cyclic voltammogram (black  
 331 line). (B) standard additions of 23.1–80.9  $\mu\text{M}$  of Chl a solutions to the real sample extracted from spinach at the potential window  
 332 with  $E_{\text{centre}} = +0.405$  V. Inset of (B): Plot of currents read at +0.49 V increase with Chl a concentration in the range of 23.1–80.9  $\mu\text{M}$   
 333 The average scan rate was 100  $\text{mVs}^{-1}$ .

#### 334 4. Conclusions

335 We have studied the electrochemical process of two chlorophyll species, Chl a and Chl b on a GC  
336 electrode based on their cyclic voltammograms and introduced a novel method for the selective detection of  
337 the individual species in the mixtures of them, using the semi-circular potential sweep voltammetry.  
338 Conventional cyclic voltammetric study revealed the similarity between the voltammograms of Chl a and  
339 Chl b, in particular, the similar peak potentials, yet failed to distinguish them in a good resolution when they  
340 are present in a mixture. The semi-circular potential wave employing the potential window with the  
341 optimised  $E_{centre}$  can selectively detect the mixtures of Chl a and Chl b in the concentration range of 46.2–111  
342  $\mu\text{M}$  and 46.2–92.4  $\mu\text{M}$ , respectively, complementing the conventional method in electroanalysis. The  
343 developed method was also successfully applied for analysing the real sample ‘spiked’ with Chl a,  
344 suggesting the potential use of semi-circular potential sweep voltammetry for the electroanalytical detection  
345 of mixtures consisting of more than one electrochemically active species with closely similar peak potentials,  
346 as the results of a simpler extraction / purification process suitable for practical use.

#### 347 Conflict of interests

348 The authors declare that they have no conflict of interest.

#### 349 Reference

- 350 Agostiano, A., Cosma, P., & Dellamonica, M. (1990). Spectroscopic and Electrochemical Characterization  
351 of Chlorophyll-a in Different Water + Organic-Solvent Mixtures. *Bioelectrochemistry and*  
352 *Bioenergetics*, 23(3), 311-324.
- 353 Amin, H. M. A., Uchida, Y., Katelhon, E., & Compton, R. G. (2019). Semi-circular potential sweep  
354 voltammetry: Experimental verification and determination of the formal potential of a reversible  
355 redox couple. *Journal of Electroanalytical Chemistry*, 836, 62-67.  
356 doi:10.1016/j.jelechem.2019.01.058
- 357 Bard, A. J., Faulkner, L. R., Zoski, C. G., & Leddy, J. (2001). *Electrochemical methods : fundamentals and*  
358 *applications* (Second edition. ed.). New York: Wiley.
- 359 Batsanov, S. S. (2001). Van der Waals radii of elements. *Inorganic Materials*, 37(9), 871-885.
- 360 Boyer, J. N., Kelble, C. R., Ortner, P. B., & Rudnick, D. T. (2009). Phytoplankton bloom status: Chlorophyll  
361 a biomass as an indicator of water quality condition in the southern estuaries of Florida, USA.  
362 *Ecological Indicators*, 9, S56-S67. doi:10.1016/j.ecolind.2008.11.013
- 363 Cecchi, T., Passamonti, P., & Cecchi, P. (2010). Study of the quality of extra virgin olive oil stored in PET  
364 bottles with or without an oxygen scavenger. *Food Chem*, 120(3), 730-735.  
365 doi:10.1016/j.foodchem.2009.11.001
- 366 Chen, L., Li, X., Tanner, E. E. L., & Compton, R. G. (2017). Catechol adsorption on graphene nanoplatelets:  
367 isotherm, flat to vertical phase transition and desorption kinetics. *Chemical Science*, 8(7), 4771-4778.
- 368 Chen, L., Tanner, E. E. L., Lin, C., & Compton, R. G. (2018). Impact electrochemistry reveals that graphene  
369 nanoplatelets catalyse the oxidation of dopamine via adsorption. *Chemical Science*, 9(1), 152-159.

- Choe, E., & Min, D. B. (2006). Mechanisms and Factors for Edible Oil Oxidation. *Comprehensive Reviews in Food Science and Food Safety*, 5(4), 169-186. doi:10.1111/j.1541-4337.2006.00009.x
- Compton, R. G., & Banks, C. E. (2018). *Understanding voltammetry* (Third Edition ed.). London: World Scientific Publishing Europe.
- Conte, L., Milani, A., Calligaris, S., Rovellini, P., Lucci, P., & Nicoli, M. C. (2020). Temperature Dependence of Oxidation Kinetics of Extra Virgin Olive Oil (EVOO) and Shelf-Life Prediction. *Foods*, 9(3). doi:10.3390/foods9030295.
- Engineering ToolBox, E. (2003). Water Content in Food and other Products. [https://www.engineeringtoolbox.com/water-content-d\\_131.html](https://www.engineeringtoolbox.com/water-content-d_131.html)
- Ergun, E., Demirata, B., Gumus, G., & Apak, R. (2004). Simultaneous determination of chlorophyll a and chlorophyll b by derivative spectrophotometry. *Analytical and Bioanalytical Chemistry*, 379(5-6), 803-811. doi:10.1007/s00216-004-2637-7
- Falk, J. E., & Smith, K. M. (1975). *Porphyrins and metalloporphyrins* (New ed.). Amsterdam ; Oxford: Elsevier.
- Goedheer, J. C., Dehaas, G. H. H., & Schuller, P. (1958). Oxidation-Reduction Potentials of Different Chlorophylls in Methanol. *Biochimica Et Biophysica Acta*, 28(2), 278-283. doi:10.1016/0006-3002(58)90474-8
- Iriyama, K., & Shiraki, M. (1979). Improved Method for Extraction, Partial-Purification, Separation and Isolation of Chlorophyll from Spinach Leaves. *Journal of Liquid Chromatography*, 2(2), 255-276.
- Isleroglu, H., Sakin-Yilmazer, M., Kemerli-Kalbaran, T., Uren, A., & Kaymak-Ertekin, F. (2017). Kinetics of colour, chlorophyll, and ascorbic acid content in spinach baked in different types of oven. *International Journal of Food Properties*, 20(11), 2456-2465.
- Khachik, F., Beecher, G. R., & Whittaker, N. F. (1986). Separation, Identification, and Quantification of the Major Carotenoid and Chlorophyll Constituents in Extracts of Several Green Vegetables by Liquid-Chromatography. *Journal of Agricultural and Food Chemistry*, 34(4), 603-616.
- Khanova, L. A., & Tarasevich, M. R. (1987). Electrochemistry and Photoelectrochemistry of Chlorophyll on a Metallic Electrode .1. Properties of Chlorophyll Adsorption Films on Metals. *Journal of Electroanalytical Chemistry*, 227(1-2), 99-114. doi: 10.1016/0022-0728(87)80068-2
- Kidmose, U., Edelenbos, M., Christensen, L. P., & Hegelund, E. (2005). Chromatographic determination of changes in pigments in spinach (*Spinacia oleracea* L.) during processing. *Journal of Chromatographic Science*, 43(9), 466-472.
- Kobayashi, M., Ohashi, S., Iwamoto, K., Shiraiwa, Y., Kato, Y., & Watanabe, T. (2007). Redox potential of chlorophyll d in vitro. *Biochimica Et Biophysica Acta-Bioenergetics*, 1767(6), 596-602.
- Lopez-Ayerra, B., Murcia, M. A., & Garcia-Carmona, F. (1998). Lipid peroxidation and chlorophyll levels in spinach during refrigerated storage and after industrial processing. *Food Chem*, 61(1-2), 113-118. doi:10.1016/S0308-8146(97)00099-X
- Maxwell, K., & Johnson, G. N. (2000). Chlorophyll fluorescence - a practical guide. *Journal of Experimental Botany*, 51(345), 659-668. doi: 10.1093/jexbot/51.345.659
- Murray, R. W. (1992). *Molecular design of electrode surfaces*. New York: Wiley.
- Nonomura, Y., Igarashi, S., Yoshioka, N., & Inoue, H. (1997). Spectroscopic properties of chlorophylls and their derivatives. Influence of molecular structure on the electronic state. *Chemical Physics*, 220(1-2), 155-166.
- Pemberton, R. M., Amine, A., & Hart, J. P. (2004). Voltammetric behavior of chlorophyll a at a screen-printed carbon electrode and its potential role as a biomarker for monitoring fecal contamination. *Analytical Letters*, 37(8), 1625-1643. doi:10.1081/Al-120037592
- Scheer, H. (1991). *Chlorophylls*. Boca Raton, Fla.: CRC Press.
- Schoefs, B. (2003). Chlorophyll and carotenoid analysis in food products. A practical case-by-case view. *Trac-Trends in Analytical Chemistry*, 22(6), 335-339. doi:10.1016/S0165-9936(03)00602-2
- Silva, S. F., Anjos, C. A. R., Cavalcanti, R. N., & Celeghini, R. M. D. (2015). Evaluation of extra virgin olive oil stability by artificial neural network. *Food Chem*, 179, 35-43. doi: 10.1016/j.foodchem.2015.01.100
- Suponeva, E. P., Hotchandani, S., Arbour, C., & Kisselev, B. A. (1996). Electrochemical oxidation of microcrystalline chlorophyll a. *Biologicheskije Membrany*, 13(3), 229-235.
- Suponeva, E. P., Kazakova, A. A., & Kisselev, B. A. (1989). Electrochemical Oxidation of Chlorophyll-a in Thin-Films at Pt and SnO<sub>2</sub> Electrodes. *Bioelectrochemistry and Bioenergetics*, 22(1), 75-81.
- Trypidis, D., Garcia-Gonzalez, D. L., Lobo-Prieto, A., Nenadis, N., Tsimidou, M. Z., & Tena, N. (2019). Real time monitoring of the combined effect of chlorophyll content and light filtering packaging on

- virgin olive oil photo-stability using mesh cell-FTIR spectroscopy. *Food Chem*, 295, 94-100. doi: 10.1016/j.foodchem.2019.05.084
- Uchida, Y., Kätelhön, E., & Compton, R. (2019). Stripping voltammetry with semi-circular potential waves: reversible systems. *Journal of Electroanalytical Chemistry*, 848, 113290.
- Uchida, Y., Katelhon, E., & Compton, R. G. (2018a). Linear sweep voltammetry with non-triangular waveforms at a microdisc electrode. *Journal of Electroanalytical Chemistry*, 823, 465-473. doi:10.1016/j.jelechem.2018.06.049
- Uchida, Y., Katelhon, E., & Compton, R. G. (2018b). Linear sweep voltammetry with non-triangular waveforms: New opportunities in electroanalysis. *Journal of Electroanalytical Chemistry*, 818, 140-148. doi:10.1016/j.jelechem.2018.04.028
- Uchida, Y., Katelhon, E., & Compton, R. G. (2019). Sweep voltammetry with a semi-circular potential waveform: Electrode kinetics. *Journal of Electroanalytical Chemistry*, 835, 60-66. doi:10.1016/j.jelechem.2018.12.030
- Vernon, L. P., & Seely, G. R. (1966). *The chlorophylls*. New York ; London: Academic Press.
- Wang, Y., Chen, L., Chaisiwamongkhol, K., & Compton, R. G. (2019). Electrochemical quantification of piperine in black pepper. *Food Chem*, 309, 125606. doi:10.1016/j.foodchem.2019.125606
- Yang, Y. G., Zhou, R. L., Han, Y. Y., & Jiang, Y. S. (1994). Electrochemical Study of Chlorophyll-a Adsorbed on SnO<sub>2</sub>. *Journal of Electroanalytical Chemistry*, 370(1-2), 269-271.
- Zhang, J., Han, W., Huang, L., Zhang, Z., Ma, Y., & Hu, Y. (2016). Leaf Chlorophyll Content Estimation of Winter Wheat Based on Visible and Near-Infrared Sensors. *Sensors (Basel)*, 16(4), 437. doi:10.3390/s16040437